SAND2017-13162J

Elsevier Editorial System(tm) for
Proceedings of The Combustion Institute
Manuscript Draft

Manuscript Number:

Title: Structure of a stratified CH4 flame with H2 addition

Article Type: 5. Turbulent Flames

Keywords: Turbulent combustion
H2 addition
Stratified flames
Multiple conditioned data analysis
Raman/Rayleigh scattering

Corresponding Author: Dr. Dirk Geyer,

Corresponding Author's Institution: Darmstadt Univ. of Applied Sciences

First Author: Silvan Schneider

Order of Authors: Silvan Schneider; Dirk Geyer; Gaetano Magnotti; Matthew J. Dunn; Robert S. Barlow; Andreas Dreizler

Abstract: To explore the effect of H2 addition (20 percent by volume) on stratified-premixed methane combustion in a turbulent flow, an experimental investigation on a new flame configuration of the Darmstadt stratified burner is conducted. Major species concentrations and temperature are measured with high spatial resolution by 1D Raman-Rayleigh scattering. A conditioning on local equivalence ratio (range from ϕ=0.45 to ϕ=1.25) and local stratification is applied to the large dataset and allows to analyze the impact of H2 addition on the flame structure. The local stratification level is determined as $\Delta\phi/\Delta T$ at the location of maximum CO mass fraction for every instantaneous flame realization. Due to the H2 addition, preferential diffusion of H2 is different than in pure methane flames. In addition to diffusing out of the reaction zone where it is formed, particularly in rich conditions, H2 also diffuses from the cold reactant mixture into the flame front. For rich conditions (ϕ=1.05 to ϕ=1.15) H2 mass fractions are significantly elevated within the intermediate temperature range compared to fully-premixed laminar flame simulations. This elevation is attributed to preferential transport of H2 into the rich flame front from adjacent richer pockets. Additionally, when the local stratification across the flame front is taken into account, it is revealed that the state-space relation of H2 is not only a function of the local stoichiometry but also the local stratification level. In these flames H2 is the only major species showing sensitivity of the state-space relation to an equivalence ratio gradient across the flame front.

Structure of a stratified CH_4 flame with H_2 addition

Silvan Schneider[1], Dirk Geyer[2], Gaetano Magnotti[3,5], Matthew J. Dunn[4], Robert S. Barlow[3], Andreas Dreizler[1]

[1]: Fachgebiet Reaktive Strömungen und Messtechnik (RSM), Technische Universität Darmstadt, Otto-Berndt-Str. 3, 64287 Darmstadt

[2]: Thermodynamik und Alternative Antriebe, Hochschule Darmstadt, Schöfferstrasse 3, 64295 Darmstadt

[3]: Sandia National Laboratories, Livermore, CA, USA

[4]: The School of Aeronautical, Mechanical and Mechatronic Engineering, University of Sydney

[5]: Clean Combustion Research Center, King Abdullah University of Science and Technology Thuwal 23955-6900, Saudi Arabia

Corresponding author:

Dirk Geyer
Email: dirk.geyer@h-da.de
FB MK
University of Applied Sciences Darmstadt
Schöfferstrasse 3
D-64295 Darmstadt

Colloquium: Turbulent Combustion

Word Count According to Method 1

Word equivalent lengths:
Main text (Introduction -> Acknowledgments) = 3686 words
Equations: 1, 15 words
Nomenclature: n/a 0 words
References: 19, 367 words
Tables: 0, 0 words

Figures and Captions:

Figure 1:	Height: 67 mm, 1 col, words including caption: 220
Figure 2:	Height: 122 mm, 1 col, words including caption: 375
Figure 3:	Height: 104 mm, 2 col, words including caption: 547
Figure 4:	Height: 35 mm, 1 col, words including caption: 152
Figure 5:	Height: 38 mm, 1 col, words including caption: 165
Figure 6:	Height: 75 mm, 1 col, words including caption: 254

Total Figures: 1713 words

Total count: 5781

Hereby we affirm that we do not intend to use color reproductions in the printed proceedings.

Abstract

To explore the effect of H_2 addition (20 percent by volume) on stratified-premixed methane combustion in a turbulent flow, an experimental investigation on a new flame configuration of the Darmstadt stratified burner is conducted. Major species concentrations and temperature are measured with high spatial resolution by 1D Raman-Rayleigh scattering. A conditioning on local equivalence ratio (range from ϕ=0.45 to ϕ=1.25) and local stratification is applied to the large dataset and allows to analyze the impact of H_2 addition on the flame structure. The local stratification level is determined as $\Delta\phi/\Delta T$ at the location of maximum CO mass fraction for every instantaneous flame realization. Due to the H_2 addition, preferential diffusion of H_2 is different than in pure methane flames. In addition to diffusing out of the reaction zone where it is formed, particularly in rich conditions, H_2 also diffuses from the cold reactant mixture into the flame front. For rich conditions (ϕ=1.05 to ϕ=1.15) H_2 mass fractions are significantly elevated within the intermediate temperature range compared to fully-premixed laminar flame simulations. This elevation is attributed to preferential transport of H_2 into the rich flame front from adjacent richer pockets. Additionally, when the local stratification across the flame front is taken into account, it is revealed that the state-space relation of H_2 is not only a function of the local stoichiometry but also the local stratification level. In these flames H_2 is the only major species showing sensitivity of the state-space relation to an equivalence ratio gradient across the flame front.

Keywords:

Turbulent combustion, H_2 addition, Stratified flames, Multiple conditioned data analysis, Raman/Rayleigh scattering

1 Introduction

Many current combustion devices such as stationary gas turbines, aero-engines and automotive engines are operated in an inhomogeneously premixed combustion regime [1]. Incomplete mixing can be intentional, e. g. to assure flame stability in global fuel-lean combustors, or it can result from practical limits on length of the mixing region. Numerous experimental and numerical studies have been conducted in stratified flames and are summarized by Lipatnikov [1] and Masri [2].

Experiments and DNS have shown significant effects of stratification on flame speed, flame topology, and internal flame structure of laminar and mildly turbulent ($u'/S_L \sim 1$) flames. When compared to homogenously premixed flames, lean stratified mixtures generally have higher flame speeds, broader reaction zones, and extended flammability limits [3,4]. These effects are attributed to enhanced fluxes of radicals and heat into the flame front. The mode of burning from a stronger lean mixture into a weaker lean mixture is referred to as 'back-supported' (e.g., Fig. 3 in [1]), while lean stratified flames with the opposite orientation are 'front supported'. For fuel-rich mixtures deductions appear more complex. Richardson et al. [5] used DNS in a turbulent slot burner and found that the burning intensity is enhanced when the flame speed in the products is faster than in the reactants. In turbulent flames the alignment of the stratification relative to the flame front can be various [6].

Significant progress has been made in recent years to quantify effects of stratification in methane flames with intermediate levels of turbulence and to test the applicability of current combustion models to turbulent stratified flames. Fiorina et al. [7] compared multiple LES approaches to simulate the turbulent stratified methane/air flames and found that flame wrinkling patterns and subgrid turbulence can be critical aspects to match experimental data. In a series of experiments on a bluff-body stabilized burner Sweeney et al. [8,9] applied multiple conditioning methods to reveal an increase of the mass fractions of H_2 and CO in a stratified environment. Thermal gradients were also increased at the location of maximum heat release. However, when a simpler level of conditioning based only on the local equivalence ratio was applied to the same data, Kamal et al. [10] concluded that the state-space relations were mainly a function of the local equivalence ratio.

The addition of H_2 generated by electrolysis from resources such as solar and wind electricity to hydrocarbon fuels offers a promising solution to accommodate for the natural fluctuations in these renewables. There have been several experimental studies of the effects of hydrogen addition in premixed turbulent methane flames [11,12]. H_2 addition increases flame speed, broadens flammability limits, and extends extinction limits. H_2 addition also adds complexity due to expected greater effects of differential diffusion. In a bluff-body stabilized premixed flames, differential diffusion of H_2 was shown to have significant effects on scalar structure [13]. To our knowledge, this is the first experimental investigation of stratified turbulent methane flames with H_2 addition based on quantitative measurements of major species and temperature. The objectives of this study are to examining the flame microstructure in temperature state-space, using conditional statistics, and determine whether effects of stratification are more significant with hydrogen addition than in normal methane flames. Differences from the findings of previous studies [8,9] in premixed and stratified methane flames are discussed.

2 Experimental Setup

2.1 Darmstadt Stratified Burner

The Darmstadt Stratified burner has been used in several experiments as well as numerical studies [6,14,15]. The geometry is described in detail in [14] and is only briefly repeated here. Three concentric tubes with inner diameters 14.8 mm (pilot), 37 mm (slot 1), and 60 mm (slot 2) are staged vertically by 5 mm for improved optical accessibility. A flame holder within the central tube stabilizes a pilot flame 40 mm upstream of the outflow. The premixed reactants from slot 1 are ignited by hot pilot flame products, and a conical turbulent flame burns outward and eventually propagates through the mixing layer formed between slot 1 and slot 2.

Several different methane hydrogen flame (MHF) configurations were generated by parametric variation of flow velocity, stoichiometry, and level of H_2 addition. In this paper only one configuration will be discussed, having unreacted bulk flow velocities of 1, 10 and 15 m/s (pilot, slot 1, slot 2) and 20 percent H_2 addition by volume of the fuel (80% CH_4) in all slots. A lean pilot flame ($\phi = 0.7$) was used. The equivalence ratio for the mixture of slot 1 ($\phi = 1.25$) and slot 2 ($\phi = 0.45$) was selected in order to

achieve identical laminar flame speeds in the mixture of slot 1, in the mean mixing layer between slot 1 and slot 2 ($\phi = 0.5(\phi_1 + \phi_2) = 0.85$), and in the fully premixed version of the flame ($\phi_1 = \phi_2 = 0.85$), which is not reported here. Laminar flame speeds of $s_{l,\phi=1.25} = s_{l,\phi=0.85} = 0.344$ m/s were derived from 1D simulations (Cantera 2.3 [16], GRI 3.0 mech. [17] including multi-component diffusion and Soret effect) at these conditions. The maximum laminar flames speed for methane with 20 percent H_2 addition is 0.434 m/s and occurs at $\phi = 1.067$.

2.2 Measurement Techniques

Multi-scalar line measurements of temperature (Rayleigh scattering) and major species (Raman scattering and CO-LIF) were performed at the Turbulent Combustion Laboratory at Sandia. The setup has been described in detail in [8,18]. 1D Raman/Rayleigh scattering was combined with two photon CO-LIF to measure species mass fractions (N_2, O_2, CH_4, H_2O, CO, CO_2, H_2) and temperature along a 6-mm segment of the combined laser beams. Four frequency doubled Nd:YAG lasers with combined 1.4 J/pulse and a beam diameter ($1/e^2$) of 220 µm were used for Raman and Rayleigh excitation. For two-photon CO LIF a 230.1-nm laser beam was employed. The scattered light was collected using an achromatic lens system and focused into a custom detection system. Non-intensified, low noise, CCD cameras were used for Raman and Rayleigh signal detection. Gating for the Raman and Rayleigh cameras (3.9 µs (FWHM) and 300 µs, respectively) was provided by custom-built rotating shutters. An intensified CCD camera was used for CO fluorescence signal detection.

For results presented here, the projected pixel spacing of the Raman/Rayleigh/CO-LIF line data was 0.02 mm along the laser axis. The optical resolution of the line-imaging system was limited to ~0.05 mm by the large-diameter, achromatic collection lens system. Effective spatial resolution can be further limited by the beam diameter and blurring caused by the flame itself.

2.3 Data Evaluation

Raman/Rayleigh/LIF data evaluation was performed using the hybrid method described in [19]. This method is based on theoretically simulated Raman spectra, except for methane where a response function based on calibrations is used. Calibration coefficients for the different species as well as normalization

curves to correct for the different throughput along the 1D probe volume were obtained by measuring several different cold flows as well as two different types of calibration flames; nearly adiabatic premixed methane/air flat flames (0.8< ϕ <1.3), and quasi-premixed hydrogen/air flames stabilized on a Hencken burner (0.2< ϕ <1.9). Representative values for precision and repeatability in scalar measurements are given in [18]. Most relevant for the present work, the precision of the temperature is 0.9% in a stoichiometric flat flame and the precision of H_2 is 6.0% in the richest CH_4/air flat flame. A spatial oversampling and wavelet denoising methodology was applied to the 1D Raman–Rayleigh-LIF data to simultaneously improve SNR and enable effective spatial resolution close to the optical resolution of the system. The wavelet denoising algorithm, termed wavelet adaptive thresholding and reconstruction (WATR), has been described in [9].

2.4 Multiple Conditioning

In order to understand the impact of hydrogen addition on space-state relations in the stratified flame, a conditioning of the single shot data on the local equivalence ratio is necessary. The local equivalence ratio was derived for each location within the 1D Raman/Rayleigh probe volume using the major species mole fractions [8]:

$$\phi = \frac{X_{CO_2}+2X_{CH_4}+X_{CO}+0.5(X_{H_2O}+X_{H_2})}{X_{CO_2}+X_{O_2}+0.5(X_{CO}+X_{H_2O})}. \quad (1)$$

As in [9] the maximum in CO mass fraction was used as a surrogate for the location of maximum heat release. The distance between maximum heat release and maximum CO mass fraction was calculated from 1D simulations and varied from 16 µm ($\phi = 0.85$) up to 60 µm ($\phi = 1.2$). In this investigation the local stratification across the flame front was quantified in terms of $\Delta\phi$ / ΔT at the location of maximum CO mass fraction. This approach has the advantage of using the temperature as a flame coordinate to normalize $\Delta\phi$ and of isolating the effects close to maximum heat release. This local stratification metric was calculated by retrieving the equivalence ratios from each instantaneous flame front measurement at the locations of $T_{Y_{\mathrm{CO,max}}}$-200 K and $T_{Y_{\mathrm{CO,max}}}$+100 K. The range of 300 K assured a robust quantification of the change in temperature.

3 Results and Discussion

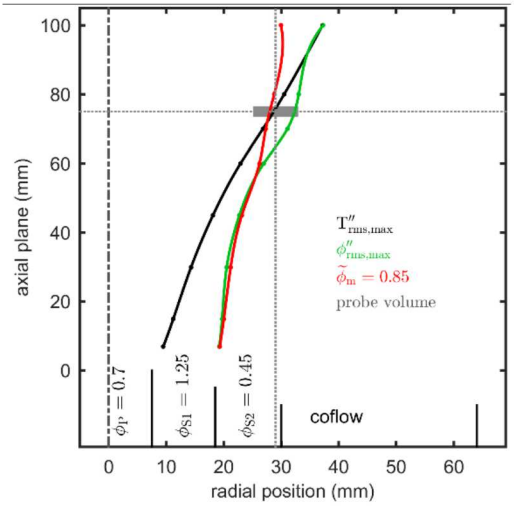

Fig. 1. Density weighted profiles of the scalar field derived from radial scans at the axial planes indicated by dots, with spline interpolation applied in between planes. The gray bar indicates the location of the probe volume for highly resolved data at intersection of flame brush ($T''_{rms,max}$) and mixing layer ($\tilde{\phi}_m = 0.85$).

Based on the findings of previous studies [8], the largest influence of stratification was expected to occur at the intersection of the mean flame brush and the mixing layer between the slots 1 and 2. The location of the mean flame brush was assessed by the density weighted maximum temperature fluctuations $T''_{rms,max}$ in each radial profile, and the center of the mixing layer by $\tilde{\phi}_m = 0.5(\phi_1 + \phi_2) = 0.85$. As illustrated in Fig. 1, the position of this intersection at $z = 75$ mm and $r = 29$ mm was derived by interpolating the radial scans through the flame. Here the 6 mm probe volume was centered (grey bar in Fig. 1), and 40,000 samples were acquired to ensure sufficient data to apply multi-conditioning.

3.1 Conditioning on equivalence ratio

Fig. 2 gives the mass fractions of the measured species (CO_2, O_2, CH_4 and H_2O) in temperature space. Data are conditioned on the local equivalence ratio. Only data where $\phi = 0.85 \pm 2.5$ % (left column) and $\phi = 1.10 \pm 2.5$ % (right column) are shown, while data in all conditioning intervals centered at $\phi = 0.65, 0.70, \ldots, 1.25$ had similar behavior. Results of unstrained and strained (1000 s^{-1}) laminar flame calculations at the corresponding equivalence ratios are included for comparison, with the effects of strain being small for shown species. CO_2, O_2, CH_4 and H_2O mass fractions agree well with laminar flame calculations for corresponding equivalence ratios. This result is consistent with the findings of Kamal et al.

[10] and indicates that local equivalence ratio is the major driver of these state-space relations, regardless of the H_2 addition in the current study.

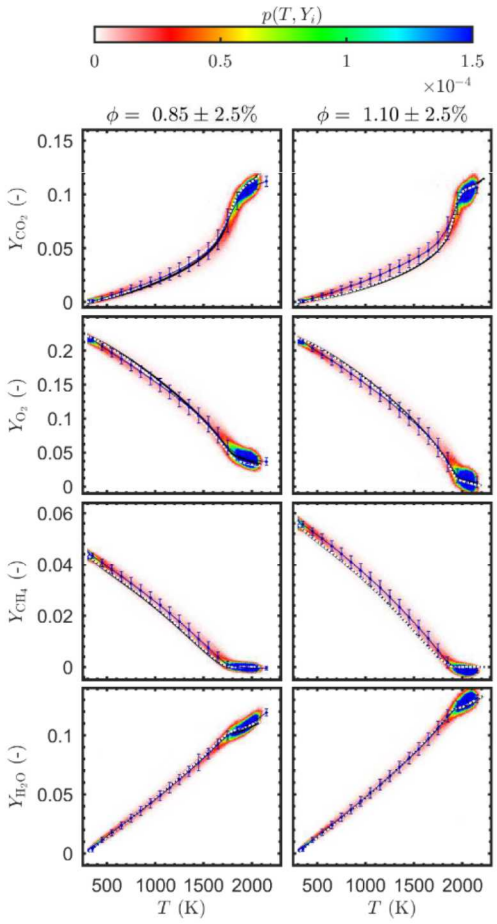

Fig. 2. Mass faction of main species (CO_2, O_2, CH_4 and H_2O) in temperature state space conditioned on the local equivalence ratio ($\phi = 0.85 \pm 2.5\%$, left; and $\phi = 1.10 \pm 2.5\%$, right). Joint probability density $p(T,Y_i)$ is color coded and represents the incidence of data at this location in the scatter plot. Mean values in each 100 K bin are plotted in blue, with vertical blue bars denoting ± one standard deviation. The laminar flame calculations are represented by black solid lines (unstrained) and white dotted lines (1000 s^{-1}).

Mass fractions of H_2 and CO are given in Fig. 3. When conditioned on lean mixtures ($\phi = 0.85 \pm 2.5\%$) the state-space relations of H_2 and CO follow the laminar flame calculations well for intermediate and high temperatures. In the low temperature region preferential diffusion of H_2 from cold mixture leads to slightly increased H_2 mass fractions. However, starting from $\phi = 1.0$ the H_2 mass fraction levels are successively elevated compared to 1D calculations in the temperature range 700 K < T < 2000 K. The greatest elevation occurs near 1650 K for $\phi = 1.1$, exhibiting an increase of the mean H_2 mass fraction by 15 %. This elevation is significant since statistical uncertainty at this location can be quantified and is much smaller than the observed elevation effect; one standard deviation of the mean estimation for Y_{H_2} is $4.6 \cdot$

10^{-6} (1600 K < T < 1700 K, $\phi = 1.1 \pm 2.5\%$, 7900 samples), while the distance of the mean to the strained 1D calculation reaches $\Delta Y_{H_2} = 4.0 \cdot 10^{-4}$. Note that the elevation of Y_{H_2} decreases in richer mixtures ($\phi > 1.1$) and ceases to exist at $\phi = 1.2$. For $\phi = 1.25$ the number of available data are too small to generate meaningful figures.

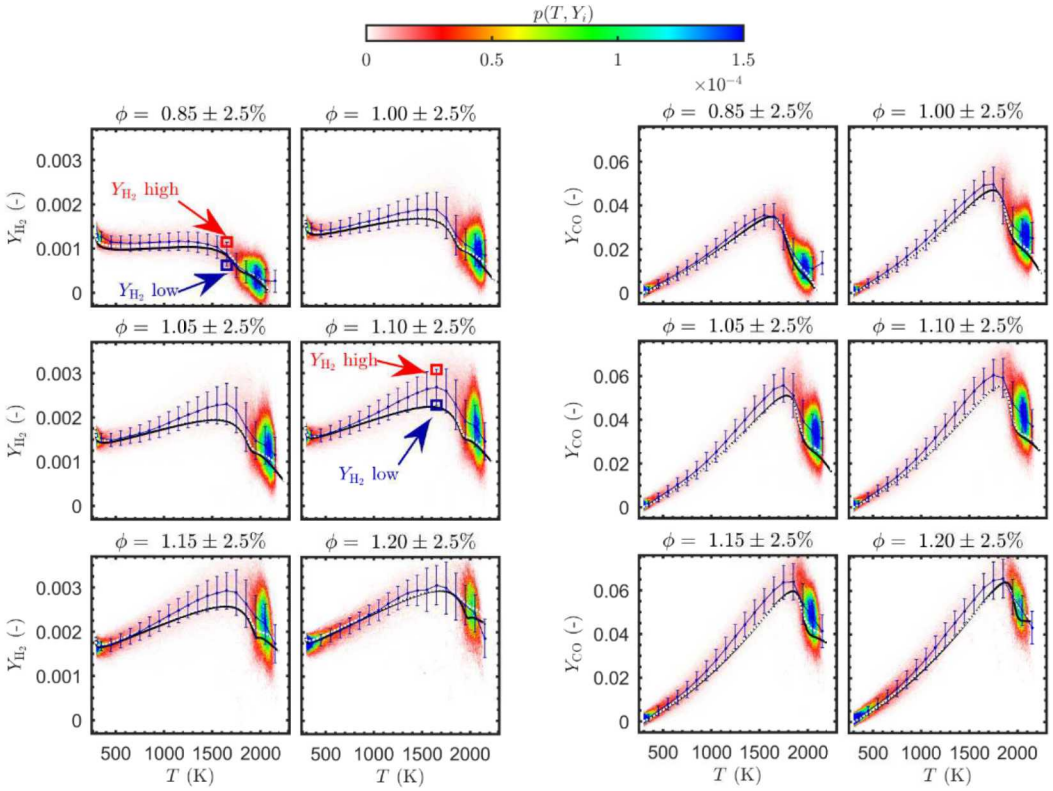

Fig. 3. Mass fraction of H_2 (left) and CO (right) conditioned on the indicated equivalence ratio intervals. Color coding of PDF and laminar flame calculations as in Fig. 2. Red and blue rectangles indicate sample regions of high and low of H_2 mass fraction, respectively.

In both experimental and computational studies of lean stratified methane flames, elevated levels of H_2 have been attributed to diffusion of H_2 from products at richer conditions (back supported flames). However, in contrast to stratified flames of just methane, H_2 addition leads to the situation where, for lean conditions, the H_2 mass fraction in the products is much lower than in the cold reactants. For results conditioned on lean values of the local equivalence ratio ($\phi = 0.85 \pm 2.5\%$ in Fig. 3 as well as leaner conditions not shown), this appears to negate the tendency for H_2 levels to be elevated by diffusion from richer mixture in lean back-supported flames. For fuel-rich laminar flames with H_2 addition the maximum Y_{H_2} levels exceed those in the reactants, and these maximum levels increase rapidly with equivalence

ratio. Therefore, the most elevated Y_{H_2} values seen in the results conditioned on $\phi = 1.0 \pm 2.5\%$ up to $\phi = 1.15 \pm 2.5\%$ are believed to result from locally high gradients in equivalence ratio (high stratification levels) as well as from the steeper increase in H_2 levels with equivalence ratio in the rich mixtures. Both drive diffusion of H_2 from adjacent richer product mixtures.

To test these hypotheses the most elevated data ($Y_{H_2} > \bar{Y}_{H_2} + 0.5 \cdot \sigma_{Y_{H_2}}$) and least elevated data ($Y_{H_2} < \bar{Y}_{H_2} - 0.5 \cdot \sigma_{Y_{H_2}}$) within the temperature range 1600 K < T < 1700 K for each of the two intervals in equivalence ratio ($\phi = 0.85 \pm 2.5\%$, $\phi = 1.10 \pm 2.5\%$), were selected for comparative analysis, as illustrated by the corresponding red and blue rectangles in Fig. 3. For each data point within these four subsets the values of equivalence ratio measured within $\pm$ 200 µm along the instantaneous 1D probe volume were sampled. Resulting populations are plotted as histograms in Fig. 4. Mean values of the equivalence ratios for these distributions are given as vertical red (blue) lines for the data from the red (blue) rectangle regions marked in Fig. 4.

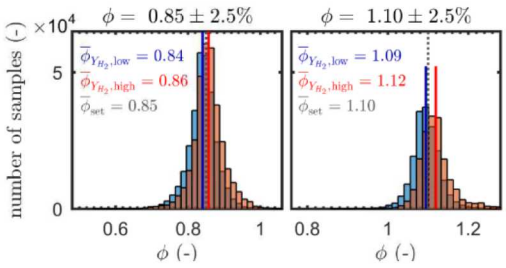

Fig. 4. Histograms of distribution of equivalence ratio in the vicinity ($\pm$ 200 µm) of the data points represented by the red and blue rectangles in Fig. 3. Means of the distributions are given as solid vertical lines (red/blue). Respective set points of ϕ (0.85 and 1.10) are marked as dotted gray line.

For the highly elevated Y_{H_2}(Fig. 4, right, red histogram) the mean of the distribution is shifted in the rich direction to $\bar{\phi} = 1.12$. This emphasizes that at the location of a high Y_{H_2}(red rectangle) the probability of the appearance of an even richer pocket in the spatial vicinity of this data point is elevated. Thus the high values of Y_{H_2} in the data conditioned on $\phi = 1.10$ can be attributed to preferential diffusion of H_2 from adjacent richer regions of the flame. The richest conditioning interval in Fig. 3 ($\phi = 1.2 \pm 2.5\%$) cannot be affected by diffusion of H_2 from significantly richer mixtures because the slot 2 flow is at $\phi = 1.25$ in this flame. Therefore no H_2 elevation is found here.

In fuel lean mixtures, represented in Fig. 4 (left) by data conditioned on $\phi = 0.85 \pm 2.5\%$, the ϕ distributions corresponding to low (blue) and high (red) Y_{H_2} are only slightly shifted from the set point of 0.85 and from each other. There is a slight tendency for high Y_{H_2} levels to be correlated with the presence of adjacent pockets at higher ϕ, but the effect is smaller than in the rich example, and there is negligible probability of finding pockets with $\phi > 1$ within the considered range of ± 200 μm. As discussed above, the levels of H_2 at low temperatures at the available adjacent mixtures exceed those at high temperatures, and this apparently reduces or eliminates the potential for differential diffusion from richer mixtures to cause H_2 elevation.

This new finding reveals that mass factions of H_2 that are higher than expected from 1D calculations appear more likely when there is a richer mixture adjacent to the flame. In locally rich mixtures state-space relations of H_2 are not only a function of the local equivalence ratio but also a function of the stoichiometry of the gas mixture in the vicinity of the flame.

In lean mixtures the CO mass fraction (Fig. 3, right) follows the 1D simulation. In rich mixtures, starting from $\phi = 1.0$ there is a slight elevation of Y_{CO} compared to laminar flame results that is similar to the observation made in pure methane flames [10]. This may be attributed to turbulence because stratification is shown in the next section to have no significant influence on Y_{CO}.

3.2 Conditioning on equivalence ratio and stratification

To further reveal the influence of stratification on the micro structure of the flame, additional conditioning is applied to the data. As outlined in Section 2.4, a measure of local stratification is calculated for each instantaneous flame front measurements as ($\Delta\phi/\Delta$T) based on the two locations corresponding to

$T_{Y_{CO,max}}$-200 K and $T_{Y_{CO,max}}$+100 K. PDFs of the measured stratification conditional on local equivalence ratio are plotted in Fig. 5.

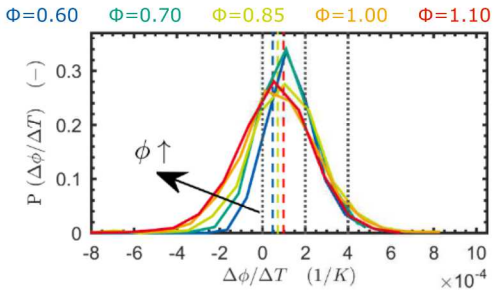

Fig. 5. Probability distribution of stratification conditioned on different local equivalence ratios ($\phi = \phi_{set} \pm 2.5\%$, color coded). Blue ($\phi = 0.6$), green ($\phi = 0.85$) and red ($\phi = 1.1$) vertical dashed lines indicate the stratification value with the used definition for a 1D strained (1000 s^{-1}) flame, respectively. Gray vertical dotted lines separate four levels of stratification as discussed in the text.

The values of stratification determined in the above manner for strained (1000 s^{-1}) 1D premixed flames are non-zero due to effects of differential diffusion on the local equivalence ratio calculated from the major species mole fractions. Calculated values for premixed flames at $\phi = 0.60, 0.85, 1.10$ are $4.8 \cdot 10^{-5}$ K^{-1}, $7.1 \cdot 10^{-5}$ K^{-1}, $9.8 \cdot 10^{-5}$ K^{-1}, respectively. These values are marked as vertical dashed lines in Fig. 5 as a comparison to the measured distributions. Number of measured samples available for the evaluation of the stratification levels in Fig. 5 are: 523 ($\phi = 0.6$), 1817 ($\phi = 0.7$), 1586 ($\phi = 0.85$), 1428 ($\phi = 1.0$) and 1180 ($\phi = 1.1$).

The average orientation of the outward-burning turbulent flame and the stratified mixing layer (Fig. 1) dictate that positive stratification ($\Delta\phi/\Delta T > 0$) should be more probable. As noted earlier, the maximum laminar flames speed occurs at $\phi = 1.067$, so positive stratification corresponds to back supported combustion for lean and stoichiometric conditions. Figure 5 shows that positive stratification is dominant for lean mixtures. However, there is a progressive shift and broadening of the pdfs with increasing ϕ. Locations of the maxima of the distributions are weakly dependent on the local equivalence ratio and located at small positive values ($0 < \Delta\phi/\Delta T < 2 \cdot 10^{-4}$ 1/K). From lean to rich mixtures the appearance of negative stratification becomes increasingly likely. This can be explained from the dependence of flame speed on equivalence ratio. Because the highest laminar flame speed occurs at $\phi = 1.067$, the lean mixtures are much weaker than the rich mixtures in the present conditional analysis. The viability of front

supported flames at the leanest condition would be very low, limiting the number of measured realization. The viability of flames with negative stratification improves with increasing ϕ, leading to the broadening of pdfs in Fig. 5 toward negative values. Note that pdfs for $\phi = 1.0$ and $\phi = 1.1$ are very similar, and these two conditions are on either side of the condition of maximum laminar flame speed.

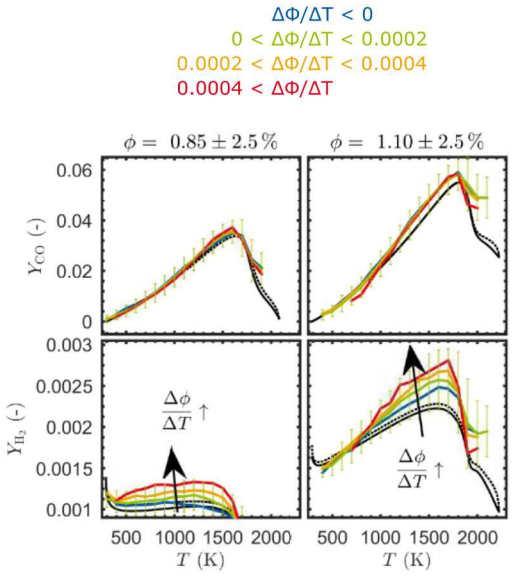

Fig. 6. Mass factions of CO and H_2 in temperature state-space conditioned on two different local equivalence ratios and four different levels of stratification (color coded). Variation of the data within a 100-K bin are given exemplary for $0 < \Delta\phi/\Delta T < 2 \cdot 10^{-4}$ 1/K as vertical bars representing one standard deviation. Laminar flame calculations are represented by black solid lines (unstrained) and grey dotted lines (1000 s^{-1}).

Figure 6 shows state space relations for H_2 and CO mass fractions conditioned on equivalence ratio and stratification level. Results reveal the insensitivity of CO levels to stratification. The main reactive species (O_2, CH_4, CO_2, H_2O) are also insensitive to the stratification level (not shown). Only the mass fraction of H_2 shows strong dependence on the level of stratification. This is true independent of the local equivalence ratio. In the temperature range 400 K < T < 1700 K Y_{H_2} is elevated due to the higher equivalence ratio of the adjacent mixture. Only highly diffusive H_2 is being transported preferentially to the preheat zone of the flame [9]. This results in higher concentrations of H_2 than expected from 1D calculations. The initial addition of H_2 to the fuel and the existence of pockets with rich mixtures make this effect much stronger than found in pure methane flames [15]. Conditioning on $\phi = 0.85 \pm 2.5\%$, (Fig. 6, left) reveals that the elevation of H_2 only occurs at positive values of stratification ($\Delta\phi/\Delta T > 2 \cdot 10^{-4}$ 1/K). The state-space relation in weakly stratified mixtures ($0 < \Delta\phi/\Delta T < 2 \cdot 10^{-4}$ 1/K) appears close to the 1D calculations.

Here, no large gradient of equivalence ratio is apparent. Thus, no source region for H_2 diffusion towards the flame front exists. In rich conditions ($\phi = 1.1 \pm 2.5\%$, Fig. 6, right) the lack of O_2 prevents the immediate reaction of H_2 and allows an elevation of Y_{H_2}. This is true also when no local stratification is present at the instant of the measurement, possibly due to history effects involving earlier diffusion of H_2 from richer mixtures. These findings reveal that in these flame conditions the state-space relation of H_2 is a function of not only the local equivalence and the stoichiometry of the gas mixture in the close vicinity ($\pm$ 200 µm) but also of the local stratification.

4 Conclusion

A turbulent stratified methane flame with 20 percent hydrogen addition, stabilized on the Darmstadt Stratified burner, has been investigated. Major species concentrations and temperature were measured at the intersection of the mean mixing layer and the flame brush to maximize the impact of stratification. These data were conditioned first on local equivalence ratio and then also on the local stratification level. The stratification level was calculated as $\Delta\phi \,/\, \Delta T$ using two points bracketing the location of maximum CO mass fraction ($T_{Y_{CO,max}}$-200 K and $T_{Y_{CO,max}}$+100 K). The location of maximum CO mass fraction was used as a surrogate for the location of maximum heat release. Thereby, the effect of equivalence ratio gradients onto the flame structure were isolated. The main findings are summarized below.

- H_2 addition leads to different preferential diffusion of H_2 than in pure methane flames.
    - In fuel lean condition H_2 diffuses from cold mixture into the flame front.
    - In rich condition H_2 diffuses out of the reaction zone where it is formed in higher concentrations than in the cold mixture.
- The state-space relations of all major species (excluding H_2 and CO) are mainly a function of local equivalence ratio thus insensitive to turbulence and stratification
- Levels of stratification are moderate. PDFs of distribution of stratification peak in mildly positively stratified flames ($\Delta\phi \,/\, \Delta T$ >0)
- CO levels are slightly elevated in rich flame regions. However, CO levels were insensitive to conditioning on the local stratification level.

- H_2 mass fractions are significantly elevated in the intermediate temperature range compared to laminar flame simulations. This is attributed to preferential transport of H_2 into the rich flame front from adjacent richer pockets and occurs if two requirements are fulfilled:
    - There is a rich mixture that lacks of O_2 for immediate reaction of H_2.
    - There is a richer mixture apparent in the close vicinity ($\pm$ 200 µm) of the probed flame front that acts as source region for diffusive H_2.
- H_2 state-space relations shows exclusive sensitivity to stratification. Higher positive stratification levels ($\Delta\phi$ / ΔT >0) lead to increasing elevation of H_2 compared to laminar flame simulations.

Acknowledgements

We gratefully acknowledge financial support by the Deutsche Forschungsgemeinschaft (DFG) through DR 374/13 and GE 2523/1. A. Dreizler was financially supported by the Gottfried Wilhelm Leibniz-Preis (DFG). Work at Sandia was supported by the United States Department of Energy, Office of Basic Energy Science, and Biosciences. Sandia National Laboratories is a multi-mission laboratory managed and operated by National Technology and Engineering Solutions of Sandia, LLC., a wholly owned subsidiary of Honeywell International, Inc., for the U.S. Department of Energy's National Nuclear Security Administration under contract DE-NA-0003525. The authors also thank Bob Harmon for his contributions to the experiments.

Figure Captions

Figure 1:

Fig. 1. Density weighted profiles of the scalar field derived from radial scans at the axial planes indicated by dots, with spline interpolation applied in between planes. The gray bar indicates the location of the probe volume for highly resolved data at intersection of flame brush ($T''_{rms,max}$) and mixing layer ($\tilde{\phi}_m = 0.85$).

Figure 2:

Fig. 2. Mass faction of main species (CO2, O2, CH4 and H2O) in temperature state space conditioned on the local equivalence ratio (φ=0.85 ±2.5%, left; and φ=1.10±2.5%, right). Joint probability density p(T,Yi) is color coded and represents the incidence of data at this location in the scatter plot. Mean values in each 100 K bin are plotted in blue, with vertical blue bars denoting ± one standard deviation. The laminar flame calculations are represented by black solid lines (unstrained) and white dotted lines (1000 s-1).

Figure 3:

Fig. 5. Mass fraction of H_2 (left) and CO (right) conditioned on the indicated equivalence ratio intervals. Color coding of PDF and laminar flame calculations as in Fig. 2. Red and blue rectangles indicate sample regions of high and low of H_2 mass fraction, respectively.

Figure 4:

Fig. 4. Histograms of distribution of equivalence ratio in the vicinity (± 200 µm) of the data points represented by the red and blue rectangles in Fig. 3. Means of the distributions are given as solid vertical lines (red/blue). Respective set points of φ (0.85 and 1.10) are marked as dotted gray line.

Figure 5:

Fig. 5. Probability distribution of stratification conditioned on different local equivalence ratios ($\phi = \phi_{set} \pm 2.5\%$, color coded). Blue ($\phi = 0.6$), green ($\phi = 0.85$) and red ($\phi = 1.1$) vertical dashed lines indicate the stratification value with the used definition for a 1D strained (1000 s^{-1}) flame, respectively. Gray vertical dotted lines separate four levels of stratification as discussed in the text.

Figure 6:

Fig. 6. Mass factions of CO and H_2 in temperature state-space conditioned on two different local equivalence ratios and four different levels of stratification (color coded). Variation of the data within a 100-K bin are given exemplary for $0 < \Delta\phi/\Delta T < 2 \cdot 10^{-4}$ 1/K as vertical bars representing one standard deviation. Laminar flame calculations are represented by black solid lines (unstrained) and grey dotted lines (1000 s^{-1}).

5 References

[1] A.N. Lipatnikov, *Prog. Energy Combust. Sci.* 62 (2017) 87–132.

[2] A.R. Masri, *Proc. Combust. Inst.* 35 (2) (2015) 1115–1136.

[3] E.S. Richardson, V.E. Granet, A. Eyssartier, J.H. Chen, *Combust. Theor. Model.* 14 (6) (2010) 775–792.

[4] R. Zhou, S. Hochgreb, *Combust. Flame* 160 (6) (2013) 1070–1082.

[5] E.S. Richardson, J.H. Chen, *Proc. Combust. Inst.* 36 (2) (2017) 1729–1736.

[6] G. Kuenne, F. Seffrin, F. Fuest, T. Stahler, A. Ketelheun, D. Geyer, J. Janicka, A. Dreizler, G. Kuenne, F. Seffrin, F. Fuest, T. Stahler, A. Ketelheun, D. Geyer, J. Janicka, A. Dreizler, *Combust. Flame* 159 (8) (2012) 2669–2689.

[7] B. Fiorina, R. Mercier, G. Kuenne, A. Ketelheun, A. Avdić, J. Janicka, D. Geyer, A. Dreizler, E. Alenius, C. Duwig, P. Trisjono, K. Kleinheinz, S. Kang, H. Pitsch, F. Proch, F. Cavallo Marincola, A. Kempf, *Combust. Flame* 162 (11) (2015) 4264–4282.

[8] M.S. Sweeney, S. Hochgreb, M.J. Dunn, R.S. Barlow, *Combust. Flame* 159 (9) (2012) 2896–2911.

[9] M.S. Sweeney, S. Hochgreb, M.J. Dunn, R.S. Barlow, *Combust. Flame* 160 (2) (2013) 322–334.

[10] M.M. Kamal, R.S. Barlow, S. Hochgreb, *Combust. Flame* 166 (2016) 76–79.

[11] R. Schefer, *Int. J. Hydrog. Energy* 28 (10) (2003) 1131–1141.

[12] H. Kim, V. Arghode, A. Gupta, *Int. J. Hydrog. Energy* 34 (2) (2009) 1063–1073.

[13] M.J. Dunn, R.S. Barlow, *Proc. Combust. Inst.* 34 (1) (2013) 1411–1419.

[14] F. Seffrin, F. Fuest, D. Geyer, A. Dreizler, *Combust. Flame* 157 (2) (2010) 384–396.

[15] T. Stahler, D. Geyer, G. Magnotti, P. Trunk, M.J. Dunn, R.S. Barlow, A. Dreizler, *Proc. Combust. Inst.* 36 (2) (2017) 1947–1955.

[16] Goodwin, D. Moffat, H., R. Speth, *Cantera: An Object-Oriented Software Toolkit For Chemical Kinetics, Thermodynamics, And Transport Processes. Version 2.3.0*, Zenodo, 2017.

[17] Gregory P. Smith, David M. Golden, Michael Frenklach, Nigel W. Moriarty, Boris Eiteneer, Mikhail Goldenberg, C. Thomas Bowman, Ronald K. Hanson, Soonho Song, William C. Gardiner, Jr., Vitali V. Lissianski, and Zhiwei Qin, *http://www.me.berkeley.edu/gri_mech/*.

[18] G. Magnotti, R.S. Barlow, *Combust. Flame* 162 (1) (2015) 100–114.

[19] F. Fuest, R.S. Barlow, D. Geyer, F. Seffrin, A. Dreizler, *Proc. Combust. Inst.* 33 (1) (2011) 815–822.